

## Hybrid simulation of collisionless shock waves using the PIC-method\*

L.V. Vshivkova, G.I. Dudnikova, T.V. Liseykina, E.A. Mesyats

**Abstract.** We present a 2D hybrid numerical plasma model for the simulation of the physical processes in supernova remnant shock precursor. In simulation, a shock is generated by sending a supersonic flow against a reflecting wall. The interaction between the incoming and reflected streams produces a sharp discontinuity, which moves away from the wall. The hybrid approach reduces computer costs relative to a fully kinetic approach while treating ions with a greater accuracy than MHD allows. Another important advantage of the hybrid approach is a possibility to study important instabilities on the ion time scale, neglecting the high-frequency modes associated with electrons. The new numerical model to investigate the processes of particle acceleration on the front of a shock wave is presented.

### 1. Introduction

In this paper, a 2D numerical model to investigate an acceleration mechanism of cosmic ray charged particles on a shock front is presented. This problem is of interest in astrophysics, plasma physics and charged particle accelerators. Numerical models, applied to the investigation of the problem of generation and dynamics of cosmic rays [1, 2], are divided into three types and are associated with the kinetic or magnetohydrodynamic approach. The most full description is based on the Vlasov kinetic equation and Maxwell's system of equations. However, the difficulty in the implementation of such a model, dealing with a big difference in space and in time scales for electrons and ions, complicates its application when carrying out computations even using modern computer systems. Also, the MHD-models are often used. Nevertheless, they do not permit the description of violation of one-flow streams when particles are reflected from the shock front. The research based on the hybrid (combined) models [3–7], where an electron component of plasma is described by the MHD-approach, while ions are kinetically treated, and vice versa [8, 9], allows one to essentially reduce the requirements for computation resources, and is now more promising in terms of numerical experiments. For their implementation, this type of models requires

---

\*The development of the new computational algorithm and calculations, including the ones using different plasma parameters, are supported by the Russian Foundation for Basic Research under Grants 14-01-31304 and 14-01-00392. The algorithm developed has been modified and optimized within the project of the Russian Science Foundation (RSF) under Grant 14-11-00485.

utilization of the PIC-method [10, 11] and the practice to solve large-scale problems based on the algorithms of parallel computations.

## 2. Statement of the problem

Let us consider a 2D-problem (in the Cartesian coordinates) of a plasma flow injection into the uniform plasma background (Figure 1). The plasma flow consists of hydrogen ions and electrons. At the initial time  $t = 0$ , the plasma

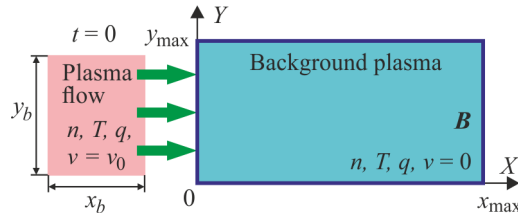


Figure 1

flow of the density  $n$ , the temperature  $T$ , the charge  $q$  and constant initial velocity  $\mathbf{v} = \mathbf{v}_0$  enters the plasma area of the uniform magnetic field  $\mathbf{B}$ , the constant density  $n$ , the temperature  $T$ , the charge  $q$ , and the velocity  $\mathbf{v} = 0$  (or  $\mathbf{v} = \mathbf{v}_0$ ).

Entering the considered area from the left, the plasma flow forms a shock wave which accelerates charged particles of the background plasma towards the right boundary and which, afterwards, are reflected from it. It is supposed that plasma is quasi-neutral, i.e. the densities of ions and electrons are equal  $n_i = n_e = n$ .

## 3. The initial system of equations

Let us write down the initial system of equations of the proposed hybrid model. The Vlasov kinetic equation for ions in the problem is solved by the PIC-method, therefore, the following characteristic equations of this kinetic equation are used

$$\frac{d\mathbf{r}}{dt} = \mathbf{v}_\alpha, \quad m_\alpha \frac{d\mathbf{v}_\alpha}{dt} = Z_\alpha e \left( \mathbf{E} + \frac{1}{c} \mathbf{v}_\alpha \times \mathbf{B} \right) + \mathbf{R}_\alpha.$$

Here  $Z_\alpha$  is the degree of ionization of ions of a sort  $\alpha$ ,  $\mathbf{E} = \{E_x, E_y, E_z\}$  and  $\mathbf{B} = \{B_x, B_y, B_z\}$  are the intensities of the electric and magnetic fields,  $\mathbf{R}_\alpha$  is the force of friction between the ions of the sort  $\alpha$  and electrons. The density  $n_\alpha$  and the average velocity of the ions  $\mathbf{V}_\alpha$  of the sort  $\alpha$  are determined by the ion distribution function  $f_\alpha$  by the velocities

$$n_\alpha = \int f_\alpha d\mathbf{v}, \quad \mathbf{V}_\alpha = \frac{1}{n_\alpha} \int f_\alpha \mathbf{v}_\alpha d\mathbf{v}.$$

The motion of an ion component of plasma is described by the magnetic hydrodynamics (MHD) approach

$$\begin{aligned}
 \frac{\partial n_e}{\partial t} + \nabla \cdot (n_e \mathbf{V}_e) &= 0, \\
 m_e \left( \frac{\partial \mathbf{V}_e}{\partial t} + (\mathbf{V}_e \cdot \nabla) \mathbf{V}_e \right) &= -e \left( \mathbf{E} + \frac{1}{c} \mathbf{V}_e \times \mathbf{B} \right) - \frac{\nabla p_e}{n_e} + \mathbf{R}_e, \\
 n_e \left( \frac{\partial T_e}{\partial t} + (\mathbf{V}_e \cdot \nabla) T_e \right) &+ (\gamma - 1) p_e \nabla \cdot \mathbf{V}_e = (\gamma - 1) (Q_e - \nabla \cdot \mathbf{q}_e),
 \end{aligned}$$

where  $n_e$ ,  $\mathbf{V}_e$  are the density and the electron velocity, respectively,  $p_e = n_e T_e$  is the electron pressure,  $\mathbf{R}_e$  is the force of friction between electrons and ions,  $T_e$  is the electron temperature,  $Q_e$  is the electron heating resulting from collisions of electrons with ions,  $\mathbf{q}_e = -\kappa_1 \nabla T_e$  is a heat flow, where  $\kappa_1$  is the heat conductivity coefficient. Also, the following Maxwell's equations are added to the system of equations:

$$\nabla \times \mathbf{B} = \frac{4\pi}{c} \mathbf{j}, \quad \nabla \times \mathbf{E} = -\frac{1}{c} \frac{\partial \mathbf{B}}{\partial t}, \quad \nabla \cdot \mathbf{B} = 0.$$

Here  $\mathbf{j}$  is the current density which in the case of multicomponent plasma is defined as  $\mathbf{j} = e(\sum_{\alpha} Z_{\alpha} n_{\alpha} \mathbf{V}_{\alpha} - n_e \mathbf{V}_e)$ , where  $\mathbf{V}_{\alpha} = (V_{\alpha x}, V_{\alpha y}, V_{\alpha z}) = (\sum_{\alpha} Z_{\alpha} n_{\alpha} \mathbf{v}_{\alpha})/n_e$  is the average ion velocity. Plasma is quasi-neutral, i.e.  $n_e = \sum_{\alpha} Z_{\alpha} n_{\alpha}$ , consequently, we do not consider the equation  $\nabla \cdot \mathbf{E} = 4\pi \rho$  in the system, where  $\rho = e(\sum_{\alpha} Z_{\alpha} n_{\alpha} - n_e)$  is a volume charge.

As the normalized values we take the following characteristic quantities: the density of the background plasma  $n_0$ , the unperturbed magnetic field  $B_0$ , the Alfvén velocity  $V_A = B_0/\sqrt{4\pi m_i n_0}$ , and the temperature  $T_0 = \frac{B_0^2}{8\pi n_0}$ .

In compliance with the stated problem, the initial conditions of the background plasma at  $t = 0$  are as follows:

$$\begin{aligned}
 n(x, y) &= n_0 = \text{const}, \quad q(x, y) = q_0 = \text{const}, \quad T(x, y) = T_0 = 0, \\
 B_x(x, y) &= B_y(x, y) = 0, \quad B_z(x, y) = B_0 = \text{const}, \\
 E_x(x, y) &= E_y(x, y) = E_z(x, y) = 0, \\
 v_x(x, y) &= v_y(x, y) = v_z(x, y) = 0.
 \end{aligned}$$

The initial conditions of the incoming flow are given as

$$\begin{aligned}
 n(x, y) &= n_0 = \text{const}, \quad q(x, y) = q_0 = \text{const}, \quad T(x, y) = T_0 = 0, \\
 v_x(x, y) &= v_0, \quad v_y(x, y) = v_z(x, y) = 0.
 \end{aligned}$$

The solution is considered in the area  $0 \leq x \leq x_{\max}$ ,  $0 \leq y \leq y_{\max}$  (see Figure 1). The boundary conditions are written down as the reflection conditions by  $x$  and the periodic conditions by  $y$  for the particles (ions); for the grid functions we have  $E_x = 0$ ,  $\partial E_y/\partial x = \partial E_z/\partial x = 0$ ,  $\partial n/\partial x = 0$ ,  $T_e = \text{const}$  by  $x$  and the periodic conditions by  $y$ .

#### 4. The algorithm description

A uniform grid with the steps  $h_x$ ,  $h_y$  by the axes  $x$  and  $y$ , respectively, is introduced in the calculation area. The grid function  $B_z$  is defined at the grid nodes  $x_i = ih_x$ ,  $y_k = kh_y$ , the grid functions  $V_x$ ,  $V_{ex}$ ,  $E_x$ ,  $B_y$ — at the nodes  $x_i$ ,  $y_{k-1/2} = (k - 0.5)h_y$ , the grid functions  $V_y$ ,  $V_{ey}$ ,  $E_y$ ,  $B_x$ — at the nodes  $x_{i-1/2} = (i - 0.5)h_x$ ,  $y_k$ , and the functions  $n$ ,  $T_e$ ,  $V_z$ ,  $V_{ez}$ ,  $E_z$ — at the centers of cells  $x_{i-1/2}$ ,  $y_{k-1/2}$ .

The equations of motion for each particle (hydrogen ions) are solved at the first computation stage:

$$v_x^{m+1} = v_x^m + \tau \left( \hat{E}_x^m + v_y^m B_z^m - v_z^m B_y^m \right), \quad (1)$$

$$v_y^{m+1} = v_y^m + \tau \left( \hat{E}_y^m + v_z^m B_x^m - v_x^m B_z^m \right), \quad (2)$$

$$v_z^{m+1} = v_z^m + \tau \left( \hat{E}_z^m + v_x^m B_y^m - v_y^m B_x^m \right), \quad (3)$$

$$x^{m+1} = x^m + \tau v_x^{m+1}, \quad y^{m+1} = y^m + \tau v_y^{m+1}. \quad (4)$$

Note, that at this stage the calculation is carried out in such a way that the terms  $\frac{\alpha \Delta_y B_z^m}{n h_y}$ ,  $-\frac{\alpha \Delta_x B_z^m}{n h_x}$  and  $\frac{\alpha}{n} \left( \frac{\Delta_x B_y^m}{h_x} - \frac{\Delta_y B_x^m}{h_y} \right)$  dealing with the friction force  $\mathbf{R}_\alpha$  are omitted in parentheses of equations (1)–(3) at first (it will be added at later in the computation). This has been made to reduce the error as these terms are canceled with similar terms in the equation for  $\mathbf{E}$ . The notation for  $\hat{E}_x$ ,  $\hat{E}_y$  and  $\hat{E}_z$  is defined below (see formulas (5)),  $m$  is a time layer number and  $\tau$  is a time step.

The ion density and the average values of the ion velocity in cells are found at the second stage:

$$n_{i-1/2, k-1/2} = \frac{1}{h_x h_y} \sum_j q_j \bar{R} \left( \frac{x_j - x_{i-1/2}}{h_x} \right) \bar{R} \left( \frac{y_j - y_{k-1/2}}{h_y} \right),$$

$$V_{i-1/2, k-1/2} = \frac{1}{n_{i-1/2, k-1/2} h_x h_y} \sum_j q_j v_j \bar{R} \left( \frac{x_j - x_{i-1/2}}{h_x} \right) \bar{R} \left( \frac{y_j - y_{k-1/2}}{h_y} \right),$$

where  $j$  is a particle number and the function  $\bar{R}$  in the PIC-method is defined as  $\bar{R}(t) = \max\{1 - |t|, 0\}$ .

Other equations of the system are solved by finite difference methods. For the sake of simplicity, the following designations are introduced in the scheme formulas:

$$\bar{f}_{x, i-1/2, k-1/2} = \frac{f_{x, i, k-1/2} + f_{x, i-1, k-1/2}}{2},$$

$$\bar{f}_{y, i-1/2, k-1/2} = \frac{f_{y, i-1/2, k} + f_{y, i-1/2, k-1}}{2},$$

$$\begin{aligned}\bar{f}_{x,i-1/2,k} &= \frac{f_{x,i,k-1/2} + f_{x,i-1,k-1/2} + f_{x,i,k+1/2} + f_{x,i-1,k+1/2}}{4}, \\ \bar{f}_{y,i,k-1/2} &= \frac{f_{y,i-1/2,k} + f_{y,i-1/2,k-1} + f_{y,i+1/2,k} + f_{y,i+1/2,k-1}}{4}, \\ \Delta_x f_{i-1/2,k-1/2} &= \begin{cases} \frac{f_{i-1/2,k-1/2} - f_{i-3/2,k-1/2}}{h_x}, & \text{if } \bar{f}_{x,i-1/2,k-1/2} > 0, \\ \frac{f_{i+1/2,k-1/2} - f_{i-1/2,k-1/2}}{h_x}, & \text{otherwise,} \end{cases} \\ \Delta_y f_{i-1/2,k-1/2} &= \begin{cases} \frac{f_{i-1/2,k-1/2} - f_{i-1/2,k-3/2}}{h_y}, & \text{if } \bar{f}_{y,i-1/2,k-1/2} > 0, \\ \frac{f_{i-1/2,k+1/2} - f_{i-1/2,k-1/2}}{h_y}, & \text{otherwise.} \end{cases}\end{aligned}$$

At the third stage, the components of the electron velocity are found:

$$\begin{aligned}V_{ex,i,k-1/2}^{m+1} &= V_{x,i,k-1/2}^{m+1} - \frac{2(B_{z,i,k}^m - B_{z,i,k-1}^m)}{h_y(n_{i-1/2,k-1/2}^{m+1} + n_{i+1/2,k+1/2}^{m+1})}, \\ V_{ey,i-1/2,k}^{m+1} &= V_{y,i-1/2,k}^{m+1} + \frac{2(B_{z,i,k}^m - B_{z,i-1,k}^m)}{h_x(n_{i-1/2,k-1/2}^{m+1} + n_{i-1/2,k+1/2}^{m+1})}, \\ V_{ez,i-1/2,k-1/2}^{m+1} &= V_{z,i-1/2,k-1/2}^{m+1} + \frac{1}{n_{i-1/2,k-1/2}^{m+1}} \times \\ &\quad \left( \frac{B_{x,i-1/2,k}^m - B_{x,i-1/2,k-1}^m}{h_y} - \frac{B_{y,i,k-1/2}^m - B_{y,i-1,k-1/2}^m}{h_x} \right).\end{aligned}$$

Before going further, let us introduce the notations of different values of the electric field intensities in the order they appear in the algorithm

$$\begin{aligned}\tilde{E}_x &= -V_{ey}B_z + V_{ez}B_y - \beta \left( \frac{\partial V_{ex}}{\partial t} + V_{ex} \frac{\partial V_{ex}}{\partial x} + V_{ey} \frac{\partial V_{ex}}{\partial y} \right), \\ \tilde{E}_y &= -V_{ez}B_x + V_{ex}B_z - \beta \left( \frac{\partial V_{ey}}{\partial t} + V_{ex} \frac{\partial V_{ey}}{\partial x} + V_{ey} \frac{\partial V_{ey}}{\partial y} \right), \\ \tilde{E}_z &= -V_{ex}B_y + V_{ey}B_x - \beta \left( \frac{\partial V_{ez}}{\partial t} + V_{ex} \frac{\partial V_{ez}}{\partial x} + V_{ey} \frac{\partial V_{ez}}{\partial y} \right), \\ E_x^* &= \tilde{E}_x + \frac{\varkappa}{n_e} \frac{\partial B_z}{\partial y} = \tilde{E}_x + \frac{\varkappa}{n} \frac{\Delta_y B_z^m}{h_y}, \\ E_y^* &= \tilde{E}_y - \frac{\varkappa}{n_e} \frac{\partial B_z}{\partial x} = \tilde{E}_y - \frac{\varkappa}{n} \frac{\Delta_x B_z^m}{h_x}, \\ E_z^* &= \tilde{E}_z + \frac{\varkappa}{n_e} \left( \frac{\partial B_y}{\partial x} - \frac{\partial B_x}{\partial y} \right) = \tilde{E}_z + \frac{\varkappa}{n} \left( \frac{\Delta_x B_y^m}{h_x} - \frac{\Delta_y B_x^m}{h_y} \right),\end{aligned}$$

$$\hat{E}_x = \tilde{E}_x - \frac{1}{2n_e} \frac{\partial p_e}{\partial x}, \quad \hat{E}_y = \tilde{E}_y - \frac{1}{2n_e} \frac{\partial p_e}{\partial y}, \quad \hat{E}_z = \tilde{E}_z, \quad (5)$$

$$E_x = E_x^* - \frac{1}{2n_e} \frac{\partial p_e}{\partial x}, \quad E_y = E_y^* - \frac{1}{2n_e} \frac{\partial p_e}{\partial y}, \quad E_z = E_z^*. \quad (6)$$

Then, at the fourth stage, preliminary values of the electric field intensities  $\tilde{E}_x$ ,  $\tilde{E}_y$ ,  $\tilde{E}_z$ ,  $E_x^*$ ,  $E_y^*$ , and  $E_z^*$  are determined:

$$\begin{aligned} \tilde{E}_{x,i,k-1/2}^{m+1} &= -\beta \left( \frac{V_{ex,i,k-1/2}^{m+1} - V_{ex,i,k-1/2}^m}{\tau} + \right. \\ &\quad V_{ex,i,k-1/2}^{m+1} \frac{V_{ex,i+1,k-1/2}^{m+1} - V_{ex,i-1,k-1/2}^{m+1}}{2h_x} + \\ &\quad \left. \overline{\overline{V}}_{ey,i,k-1/2}^{m+1} \frac{V_{ex,i,k+1/2}^{m+1} - V_{ex,i,k-3/2}^{m+1}}{2h_y} \right) - \\ &\quad \overline{\overline{V}}_{ey,i,k-1/2}^{m+1} \frac{B_{z,i,k}^m + B_{z,i,k-1}^m}{2} + \\ &\quad B_{y,i,k-1/2}^m \frac{V_{ez,i+1/2,k-1/2}^{m+1} + V_{ez,i-1/2,k-1/2}^{m+1}}{2}, \\ \tilde{E}_{y,i-1/2,k}^{m+1} &= -\beta \left( \frac{V_{ey,i-1/2,k}^{m+1} - V_{ey,i-1/2,k}^m}{\tau} + \right. \\ &\quad \overline{\overline{V}}_{ex,i-1/2,k}^{m+1} \frac{V_{ey,i+1/2,k}^{m+1} - V_{ey,i-3/2,k}^{m+1}}{2h_x} + \\ &\quad \left. V_{ey,i-1/2,k}^{m+1} \frac{V_{ey,i-1/2,k+1}^{m+1} - V_{ey,i-1/2,k-1}^{m+1}}{2h_y} \right) - \\ &\quad B_{x,i-1/2,k}^m \frac{V_{ez,i-1/2,k+1/2}^{m+1} + V_{ez,i-1/2,k-1/2}^{m+1}}{2} + \\ &\quad \overline{\overline{V}}_{ex,i-1/2,k}^{m+1} \frac{B_{z,i,k}^m + B_{z,i-1,k}^m}{2}, \\ \tilde{E}_{z,i-1/2,k-1/2}^{m+1} &= -\beta \left( \frac{V_{ez,i-1/2,k-1/2}^{m+1} - V_{ez,i-1/2,k-1/2}^m}{\tau} + \right. \\ &\quad \frac{V_{ex,i,k-1/2}^{m+1} + V_{ex,i-1,k-1/2}^{m+1}}{2} \frac{V_{ez,i+1/2,k-1/2}^{m+1} - V_{ez,i-3/2,k-1/2}^{m+1}}{2h_x} + \\ &\quad \left. \frac{V_{ey,i-1/2,k}^{m+1} + V_{ey,i-1/2,k-1}^{m+1}}{2} \frac{V_{ez,i-1/2,k+1/2}^{m+1} - V_{ez,i-1/2,k-3/2}^{m+1}}{2h_y} \right) - \\ &\quad \frac{B_{y,i,k-1/2}^m + B_{y,i-1,k-1/2}^m}{2} \frac{V_{ex,i,k-1/2}^{m+1} + V_{ex,i-1,k-1/2}^{m+1}}{2} + \end{aligned}$$

$$\begin{aligned}
& \frac{B_{x,i-1/2,k}^m + B_{x,i-1/2,k-1}^m}{2} \frac{V_{ey,i-1/2,k}^{m+1} + V_{ey,i-1/2,k-1}^{m+1}}{2}, \\
E_{x,i,k-1/2}^{*m+1} &= \tilde{E}_{x,i,k-1/2}^{m+1} + \frac{2\alpha(B_{z,i,k}^m - B_{z,i,k-1}^m)}{(n_{i+1/2,k-1/2}^{m+1} + n_{i-1/2,k-1/2}^{m+1})h_y}, \\
E_{y,i-1/2,k}^{*m+1} &= \tilde{E}_{y,i-1/2,k}^{m+1} - \frac{2\alpha(B_{z,i,k}^m - B_{z,i-1,k}^m)}{(n_{i-1/2,k+1/2}^{m+1} + n_{i-1/2,k-1/2}^{m+1})h_x}, \\
E_{z,i-1/2,k-1/2}^{*m+1} &= \tilde{E}_{z,i-1/2,k-1/2}^{m+1} + \frac{\alpha}{n_{i-1/2,k-1/2}^{m+1}} \left( \frac{B_{y,i,k-1/2}^m - B_{y,i-1,k-1/2}^m}{h_x} - \frac{B_{x,i-1/2,k}^m - B_{x,i-1/2,k-1}^m}{h_y} \right).
\end{aligned}$$

At the fifth stage, the magnitudes of the magnetic field intensities are computed:

$$\begin{aligned}
B_{x,i-1/2,k}^{m+1} &= B_{x,i-1/2,k}^m - \frac{\tau(E_{z,i-1/2,k+1/2}^{*m+1} - E_{z,i-1/2,k-1/2}^{*m+1})}{h_y}, \\
B_{y,i,k-1/2}^{m+1} &= B_{y,i,k-1/2}^m + \frac{\tau(E_{z,i+1/2,k-1/2}^{*m+1} - E_{z,i-1/2,k-1/2}^{*m+1})}{h_x}, \\
B_{z,i,k}^{m+1} &= B_{z,i,k}^m + \tau \left( \frac{E_{x,i,k+1/2}^{*m+1} - E_{x,i,k-1/2}^{*m+1}}{h_y} - \frac{E_{y,i+1/2,k}^{*m+1} - E_{y,i-1/2,k}^{*m+1}}{h_x} \right) + \tilde{P}_{i,k},
\end{aligned}$$

where  $\tilde{P}_{i,k} = -\frac{\tau}{2} \left[ \frac{\partial}{\partial y} \left( \frac{1}{n_e} \frac{\partial(n_e T_e)}{\partial x} \right) - \frac{\partial}{\partial x} \left( \frac{1}{n_e} \frac{\partial(n_e T_e)}{\partial y} \right) \right]_{i,k}$  or

$$\begin{aligned}
\tilde{P}_{i,k} &= -\frac{\tau}{4h_x h_y} \frac{1}{\bar{n}_{i,k}^{m+1}} \times \\
& \left[ (n_{i+1/2,k+1/2}^{m+1} - n_{i-1/2,k-1/2}^{m+1})(T_{i-1/2,k+1/2}^m - T_{i+1/2,k-1/2}^m) + \right. \\
& \left. (n_{i+1/2,k-1/2}^{m+1} - n_{i-1/2,k+1/2}^{m+1})(T_{i+1/2,k+1/2}^m - T_{i-1/2,k-1/2}^m) \right].
\end{aligned}$$

Also, let us note that the pressure  $p_{i,k}$  in terms of  $\tilde{P}_{i,k}$  is  $p_{i,k} = \bar{n}_{i,k} \tilde{P}_{i,k}$ . Here, in order to calculate the term  $\nabla n \cdot \nabla T_e$  more accurately, the corresponding terms in the calculation formulas for  $B_z$  are taken from the formulas for  $\mathbf{E}$ . From their combination, the term  $\tilde{P}_{i,k}$  appears, and the terms  $E^*$  are used instead of  $E$  in the formulas for  $B_z$ . This way increases the stability of the scheme.

Afterwards, at the sixth stage, we find  $\hat{E}_x$ ,  $\hat{E}_y$ ,  $\hat{E}_z$  and then determine the final values of the electric field intensities  $E_x$ ,  $E_y$ ,  $E_z$  using formulas (5) and (6). Consequently, we have

$$\begin{aligned}
E_{x,i,k-1/2}^{m+1} &= E_{x,i,k-1/2}^{*m+1} - \frac{1}{2h_x} \left[ T_{i+1/2,k-1/2}^m - T_{i-1/2,k-1/2}^m + \right. \\
&\quad \left. (T_{i+1/2,k-1/2}^m + T_{i-1/2,k-1/2}^m) \frac{n_{i+1/2,k-1/2}^{m+1} - n_{i-1/2,k-1/2}^{m+1}}{n_{i+1/2,k-1/2}^{m+1} + n_{i-1/2,k-1/2}^{m+1}} \right], \\
E_{y,i-1/2,k}^{m+1} &= E_{y,i-1/2,k}^{*m+1} - \frac{1}{2h_y} \left[ T_{i-1/2,k+1/2}^m - T_{i-1/2,k-1/2}^m + \right. \\
&\quad \left. (T_{i-1/2,k+1/2}^m + T_{i-1/2,k-1/2}^m) \frac{n_{i-1/2,k+1/2}^{m+1} - n_{i-1/2,k-1/2}^{m+1}}{n_{i-1/2,k+1/2}^{m+1} + n_{i-1/2,k-1/2}^{m+1}} \right].
\end{aligned}$$

Finally, at the seventh stage of computation we determine the temperature  $T$  using the splitting scheme, each step being implemented by an implicit scheme to improve its stability. Also, the velocity sign was taken into account:

$$\begin{aligned}
T_{i-1/2,k-1/2}^{m+1/2} &= T_{i-1/2,k-1/2}^m - \tau \bar{V}_{ex,i-1/2,k-1/2}^{m+1} \Delta_x T_{i-1/2,k-1/2}^{m+1/2} - \\
&\quad \tau(\gamma - 1) T_{i-1/2,k-1/2}^m \left( \frac{V_{ex,i,k-1/2}^{m+1} - V_{ex,i-1,k-1/2}^{m+1}}{h_x} + \right. \\
&\quad \left. \frac{V_{ey,i-1/2,k}^{m+1} - V_{ey,i-1/2,k-1}^{m+1}}{h_y} \right) + \frac{2\tau \alpha (\gamma - 1)}{(n_{i-1/2,k-1/2}^{m+1})^2} \times \\
&\quad \left[ \frac{1}{h_y^2} (B_{z,i,k}^{m+1} + B_{z,i-1,k}^{m+1} - B_{z,i,k-1}^{m+1} - B_{z,i-1,k-1}^{m+1})^2 + \right. \\
&\quad \left. \frac{1}{h_x^2} (B_{z,i,k}^{m+1} + B_{z,i,k-1}^{m+1} - B_{z,i-1,k}^{m+1} - B_{z,i-1,k-1}^{m+1})^2 + \right. \\
&\quad \left. \left( \frac{B_{y,i,k-1/2}^{m+1} - B_{y,i-1,k-1/2}^{m+1}}{h_x} - \frac{B_{x,i-1/2,k}^{m+1} - B_{x,i-1/2,k-1}^{m+1}}{h_y} \right)^2 \right] + \\
&\quad \frac{\tau \alpha_1 (\gamma - 1)}{n_{i-1/2,k-1/2}^{m+1} h_x^2} \left( T_{i+1/2,k-1/2}^{m+1/2} - 2T_{i-1/2,k-1/2}^{m+1/2} + T_{i-3/2,k-1/2}^{m+1/2} \right), \\
T_{i-1/2,k-1/2}^{m+1} &= T_{i-1/2,k-1/2}^{m+1/2} - \tau \bar{V}_{ey,i-1/2,k-1/2}^{m+1} \Delta_y T_{i-1/2,k-1/2}^{m+1} + \\
&\quad \frac{\tau \alpha_1 (\gamma - 1)}{n_{i-1/2,k-1/2}^{m+1} h_y^2} \left( T_{i-1/2,k+1/2}^{m+1} - 2T_{i-1/2,k-1/2}^{m+1} + T_{i-1/2,k-3/2}^{m+1} \right).
\end{aligned}$$

The algorithm proposed has the first approximation order with respect to time and space.

## 5. Computational results

Let us consider the computational results of the wave oscillation formation when the plasma flow with the velocity  $\mathbf{v} = \mathbf{v}_0$  enters the area of unperturbed

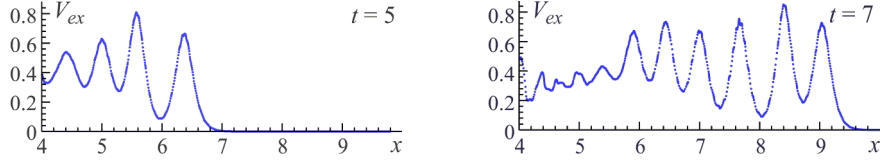


**Figure 2.** Particle phase planes at the different instants time

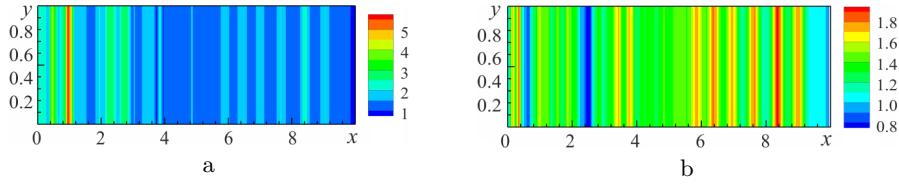


**Figure 3.** Isolines of the plasma density (a) and  $z$ -component of the magnetic field  $B_z$  (b)

plasma. Here the electron temperature was taken to be zero, i.e.  $T_e = 0$ . All the results are presented in dimensionless variables.

Figure 2 shows the particle distribution on the phase planes for different time instants. The velocity of the incoming flow is  $v_0 = 1$ . As we can see from this graph, the formed wave has a regular oscillation structure with a characteristic oscillation scale equal to 0.5. The wave distribution velocity is  $1.3V_A$ . The isolines of the plasma density and  $z$ -component of the magnetic field  $B_z$  are illustrated in Figure 3 at the time instant  $t = 7$  for the above parameters. In these figures, one can see the coincidence of the maximum value coordinates for the density and the magnetic field resulting from the condition of infinite plasma conductivity chosen for this run. An increase in the incoming flow velocity up to  $v_0 = 4$  brings about the shock wave formation, and as a result of its propagation the particles are reflected from its front. The particle distribution at the time instant  $t = 3, 4.2,$  and  $4.6$  is given in Figure 4. Here the velocity of the shock wave propagation is  $2.4V_A$ , and the velocity of the reflected particles is of order up to 5. The formation of the “step” on the shock wave front is caused by the Larmor rotation of the reflected particles under the effect of the magnetic field.

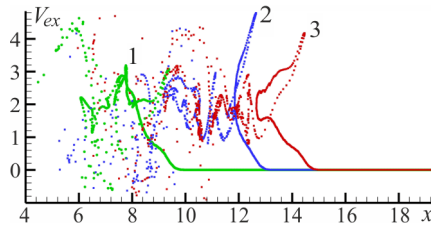


**Figure 4.** Particle phase planes at the time instants  $t = 3$  (1),  $4.2$  (2), and  $4.6$  (3)

Thus, the developed numerical model permits one to describe the shock formation processes for different Mach numbers of the incoming flow and the particle reflection from the shock front, whose velocities can attain  $v = 2v_{\text{shock wave}}$ .

**References**

- [1] Riquelme M.A., Spitkovsky A. Magnetic amplification by magnetized cosmic rays in supernova remnant shocks // *J. Astrophys.* — 2010. — Vol. 717. — P. 1054–1066.
- [2] Caprioli D., Spitkovsky A. Cosmic-ray-induced filamentation instability in collisionless shocks // *J. Lett. Astrophys.* — 2013. — Vol. 765. — doi:10.1088/2041-8205/765/1/L20.
- [3] Berezin Yu.A., Vshivkov V.A., Dudnikova G.I., Fedoruk M.P. About collisionless deceleration of the plasma cloud in the inhomogeneous magnetized background // *Plasma Physics.* — 1992. — Vol. 18, No. 12. — P. 1567–1574 (In Russian).
- [4] Vshivkov V.A., Dudnikova G.I. Kinetic-hydrodynamic models of the dynamics of interpenetrating plasma flows // *Modeling in Mechanics.* — 1990. — Vol. 4 (21), No. 1. — P. 93–97 (In Russian).
- [5] Lipatov A.S. *The Hybrid Multiscale Simulation Technology. An Introduction with Application to Astrophysical and Laboratory Plasmas.* — Berlin, Heidelberg: Springer, 2002.
- [6] Vshivkova L.V. Numerical modeling of the multi-component plasma dynamics // *Bulletin of the Novosibirsk State University.* — 2003. — Vol. 3, No. 2. — P. 3–20 (In Russian).
- [7] Vshivkova L.V., Dudnikova G.I. Dispersion analysis of the hybrid plasma model // *Bull. of the Novosibirsk Comp. Center. Series: Numerical Analysis.* — 2013. — Iss. 16. — P. 101–106.
- [8] Vshivkova L.V. Numerical simulation of plasma using the hybrid MHD-kinetic model // *Bull. of the Novosibirsk Comp. Center. Series: Numerical Analysis.* — 2009. — Iss. 14. — P. 95–114.
- [9] Vshivkova L.V., Dudnikova G.I. Numerical modeling of plasma phenomena using the PIC-method // *IEEE Conf. Publ. 25th Int. Symp. Disch. El. Ins. Vac. (ISDEIV).* — 2012. — P. 398–400.
- [10] Berezin Yu.A., Vshivkov V.A. *Particle-in-Cell Method in the Dynamics of Low-Density Plasma.* — Novosibirsk: Nauka, 1980 (In Russian).
- [11] Grigoryev Yu.N., Vshivkov V.A., Fedoruk M.P. *Numerical Particle-in-Cell Methods: Theory and Applications.* — De Gruyter, 2002.